JOURNAL OF BACTERIOLOGY, July 2007, p. 5325–5333 Vol. 189, No. 14
0021-9193/07/$08.00+0 doi:10.1128/JB.00481-07

Identification of Regions Critically Affecting Kinetics and Allosteric Regulation of the *Escherichia coli* ADP-Glucose Pyrophosphorylase by Modeling and Pentapeptide-Scanning Mutagenesis▽

Miguel A. Ballicora,[1]* Esteban D. Erben,[2]† Terutaka Yazaki,[3] Ana L. Bertolo,[3]‡ Ana M. Demonte,[2] Jennifer R. Schmidt,[3] Mabel Aleanzi,[2] Clarisa M. Bejar,[3] Carlos M. Figueroa,[2] Corina M. Fusari,[2]§ Alberto A. Iglesias,[2] and Jack Preiss[3]

Department of Chemistry, Loyola University, Chicago, Illinois 60626[1]; Laboratorio de Enzimología Molecular, Cátedra de Bioquímica Básica de Macromoléculas, Facultad de Bioquímica y Ciencias Biológicas, Universidad Nacional del Litoral, Santa Fe, Argentina[2]; and Department of Biochemistry and Molecular Biology, Michigan State University, East Lansing, Michigan 48824[3]

Received 29 March 2007/Accepted 30 April 2007

ADP-glucose pyrophosphorylase (ADP-Glc PPase) is the enzyme responsible for the regulation of bacterial glycogen synthesis. To perform a structure-function relationship study of the *Escherichia coli* ADP-Glc PPase enzyme, we studied the effects of pentapeptide insertions at different positions in the enzyme and analyzed the results with a homology model. We randomly inserted 15 bp in a plasmid with the ADP-Glc PPase gene. We obtained 140 modified plasmids with single insertions of which 21 were in the coding region of the enzyme. Fourteen of them generated insertions of five amino acids, whereas the other seven created a stop codon and produced truncations. Correlation of ADP-Glc PPase activity to these modifications validated the enzyme model. Six of the insertions and one truncation produced enzymes with sufficient activity for the *E. coli* cells to synthesize glycogen and stain in the presence of iodine vapor. These were in regions away from the substrate site, whereas the mutants that did not stain had alterations in critical areas of the protein. The enzyme with a pentapeptide insertion between Leu^{102} and Pro^{103} was catalytically competent but insensitive to activation. We postulate this region as critical for the allosteric regulation of the enzyme, participating in the communication between the catalytic and regulatory domains.

The biosynthesis of glycogen is an important strategy for storage of energy and carbon surplus. It has been suggested that the accumulation of glycogen in bacteria may give advantages under starvation periods (55). The precise role of bacterial glycogen is not completely clear, but its synthesis has been associated with several processes, such as sporulation, differentiation, growth, cariogenesis, biofilm formation, and virulence (reviewed in reference 3). Here, with computational and insertion mutagenesis studies, we sought to find important regulatory regions in the enzyme that controls bacterial glycogen metabolism.

Synthesis of bacterial glycogen uses ADP-glucose (ADP-Glc) as the glucosyl donor for the elongation of the α-1,4-glucosidic chain (29). The main regulatory step takes place at the level of ADP-Glc synthesis, which is the first committed step of the pathway (3) and is catalyzed by ADP-Glc pyrophosphorylase (ADP-Glc PPase) (ATP:α-D-glucose-1-phosphate [Glc1P] adenylyltransferase) (EC 2.7.7.27): ATP + Glc1P ⇔ ADP-Glc + PP_i.

The reaction is freely reversible in vitro, but in the cell, the hydrolysis of PP_i and the use of the sugar nucleotide make it practically irreversible in the direction of ADP-Glc synthesis (29). Small effector molecules allosterically regulate most of the ADP-Glc PPases. The activators are generally key metabolites that signal the presence of high carbon and energy levels within the cell. Hence, when carbon and energy are in excess, the synthesis of bacterial glycogen is maximal (29). The importance of the regulation of ADP-Glc PPase for the synthesis of glycogen is illustrated by the direct relationship between the affinity of this enzyme for the activator, fructose-1,6-bisphosphate (FBP), and the ability of the cell to accumulate glycogen (46).

The allosteric behavior of this enzyme is very well documented (3), but its mechanism is still unknown and the regions responsible are not clearly identified. The ADP-Glc PPase from gram-negative bacteria is a homotetramer (α_4), in which each monomer is ~50 kDa with two predicted domains (3). A residue in the N terminus (Lys^{39}) contributes to the binding of FBP (17), but ~150 residues of the C terminus are responsible for activator selectivity (5). Recently, we found that these two putative N and C domains interact strongly when they were coexpressed as separate polypeptides (6).

Information about the arrangement of the N and C domains would be crucial to understand the regulation of the ADP-Glc PPase and bacterial glycogen synthesis. There are current ef-

* Corresponding author. Mailing address for Miguel A. Ballicora: Department of Chemistry, Loyola University, Chicago, IL 60626. Phone: (773) 508-3154. Fax: (773) 508-3086. E-mail: mballic@luc.edu. Mailing address for Jack Preiss: Dept. of Biochemistry & Molecular Biology, Michigan State University, E. Lansing, MI 48824. Phone: (517)353-3137. Fax: (517)353-9334. E-mail: preiss@msu.edu.

† Present address: INGEBI, Vuelta de Obligado 2490, 1428 Buenos Aires, Argentina.

‡ Present address: Departamento de Genética, Escola Superior de Agricultura "Luiz de Queiroz," Universidade de São Paulo, Av. Pádua Dias 11, CP 83, CEP 13400-970, Piracicaba, SP, Brazil.

§ Present address: INTA, Castelar, Pcia. de Buenos Aires, Argentina.

▽ Published ahead of print on 11 May 2007.

forts to obtain a three-dimensional structure of a bacterial ADP-Glc PPase (11), but its atomic coordinates are not available yet. However, there are several crystal structures of other nucleoside diphosphate sugar pyrophosphorylases (NDP-sugar PPase), and recently, the structure of an inhibited form of the small (S) subunit of a plant ADP-Glc PPase became available (30). Here, we develop a homology model for *Escherichia coli* ADP-Glc PPase and use it to predict important regulatory regions by pentapeptide-scanning mutagenesis. This mutagenesis technique introduces a single fragment of five amino acids at a random position in a protein (25). The local structure compromised by the enzyme activity would be more likely altered by this type of mutagenesis (short insertions) rather than by single point mutations. In general, insertions in surface-exposed loops are less harmful than insertions in α-helices or β-sheets. However, insertions in loops close to the active site also have very serious effects on protein function. Analysis of the position of the insertion and their phenotypic differences has provided important structure-function relationship information for proteins with either known, modeled, or unknown structure (1, 6, 9, 15, 24, 44). In this study, we analyze the kinetic properties of *E. coli* ADP-Glc PPase mutants that contained different pentapeptide insertions to locate important regions involved in kinetics and allosteric regulation.

MATERIALS AND METHODS

Materials. α-D-[U-^{14}C]glucose-1-phosphate was purchased from Amersham Pharmacia Biotech (Piscataway, NJ). $^{32}PP_i$ was purchased from NEN Life Science Products (Boston, MA). Glc1P, ATP, ADP-Glc, and inorganic pyrophosphatase were purchased from Sigma Chemical Co. (St. Louis, MO). All other reagents were purchased at the highest quality available.

Mutagenesis. Random insertion of a single 15-bp fragment per plasmid (pETEC) was performed by the method of Hayes et al. (24) as modified by Biery et al. (7) with the commercial GPS-LS linker-scanning system from New England Biolabs. We followed directions according to the manufacturer with some modifications. The 15-bp fragment comprises 10 bp left by a transposon and 5 bp duplicated from the plasmid at the site of the insertion. This 15 bp could insert in any of the three possible frames. The acceptor plasmid, pETEC, is a derivative of pET24a (Novagen) with the *E. coli* ADP-Glc PPase gene subcloned between NdeI and SacI restriction sites (5). We incubated pETEC with the ori$^-$ transprimer donor (pGPS4) and transposase to introduce a single copy of a transposon (Transprimer, consisting a cassette with a 15-nucleotide fragment flanked by transposable elements) with resistance to chloramphenicol. With this reaction mixture, we transformed *E. coli* XL1-Blue cells (Stratagene) and obtained 140 colonies resistant to both kanamycin and chloramphenicol. Plasmid DNA was extracted from each colony, digested with NdeI and SacI, and analyzed by agarose gel electrophoresis. We selected 23 colonies that yielded plasmids with a ~2.7-kb NdeI-SacI fragment: ~1.4-kb transprimer plus ~1.3-kb ADP-Glc PPase coding region. Colonies yielding ~1.3-kb fragments were discarded. The inserted transprimer contained two flanking PmeI sites. To remove it, the selected plasmids were digested with PmeI and religated. After this step, only the 15-bp fragment remained inserted in the plasmids. These constructs were transformed into XL1-Blue cells, and kanamycin-resistant/chloramphenicol-sensitive (non-transprimer-containing) colonies were picked. Plasmids were purified and digested with PmeI and ApaI restriction enzymes (PmeI cuts in the insertion, and ApaI cuts ~1 kb upstream of the NdeI site). Agarose gel electrophoresis analysis allowed us to map the insertions and verify that a single copy was introduced in the gene. Localization of the 15-bp inserts was further confirmed by DNA sequencing. Two plasmids were discarded because they did not contain 15-bp insertions in the ADP-Glc PPase coding region. Twenty-one colonies were selected for expression and further analysis of the mutated ADP-Glc PPase genes.

Structure prediction analysis. Secondary structures were predicted with the PHD program (49) and the PSIPRED method (32), available on the Predictprotein server (http://www1.embl-heidelberg.de/Services/sander/predictprotein/) and on the PSIPRED server (38) (http://bioinf.cs.ucl.ac.uk/psipred/), respectively. Threading analysis and fold recognition was performed with the GenTHREADER program (31, 39) and by comparison to a library of hidden Markov models on the Superfamily server (20) (http://supfam.org). E values returned by these methods were the theoretically expected number of false hits per sequence query.

In the initial steps of homology modeling, we used the SWISS-MODEL server (23, 53) (http://www.expasy.ch/swissmod) and the program Modeler 7v7 for the final models (51). The known atomic coordinates of chain A of the dTDP-glucose pyrophosphorylase (dTDP-Glc PPase) (dTTP:α-D-glucose-1-phosphate thymidylyltransferase) (EC 2.7.7.24) from *E. coli* complexed with thymidine and Glc1P (Protein Data Bank accession number 1H5R) and complexed with dTTP and Mg^{2+} (accession number 1MC3) were used as templates. Ligands Glc1P and deoxyribose triphosphate were modeled from accession numbers 1H5R and 1MC3, respectively, using Modeler 7v7. Deoxyribose triphosphate is the common moiety between dTTP and ATP, substrates of the template and the target, respectively. Sequence alignment was performed manually considering information gathered from prediction of secondary structure, hydrophobic clusters, and conserved residues among the NDP-sugar PPase family (3, 16). We avoided gaps in secondary structure elements and in buried regions (52). In loops, deletions were placed between residues of the template that are close in space (31, 49). The model was checked with three-dimensional profiles using the program Verify3D (12) (http://www.doe-mbi.ucla.edu/Services/Verify_3D/), and the alignment was corrected iteratively according to the profiles. The Ramachandran plot (48) of the model was checked with the program PROCHECK (35) (http://biotech.embl-ebi.ac.uk:8400/).

A model of the *E. coli* ADP-Glc PPase based on the structure of the S subunit from the potato tuber ADP-Glc PPase was built using as template the known coordinates of the monomer complexed to ATP (chain C of the structure given accession number 1YP3 deposited in the Protein Data Bank). Loops between residues 427 to 431 and 369 to 372 were further refined with the program MODLOOP (13, 14). In the models based on the dTDP-Glc PPase and on the ADP-Glc PPase from potato tuber, we considered that the loop between residues Pro^{260} and Ala^{270} was not reliable because insertions longer than eight residues are generally not possible to model with confidence with the current methods (52). However, this loop was far from the insertions and the important regions analyzed in this work. Pictures of models were prepared with the program DeepView Swiss-PdbViewer (www.expasy.org/spdbv/) (23). Pictures were labeled and rendered with the program POV-Ray (www.povray.org).

DNA methods. The Macromolecular Structure, Sequencing, and Synthesis Facility at Michigan State University performed the automated DNA sequencing.

Protein methods. Protein concentration during enzyme purification was measured by using bicinchoninic acid reagent (54) from Pierce Chemical Company (Rockford, IL), with bovine serum albumin as the standard. Interfering substances were removed by precipitation (2).

Expression and purification of mutant enzymes. For expression of the wild-type and mutated ADP-Glc PPases, *E. coli* BL21(DE3) cells (Novagen) were transformed with pETEC or its mutated derivatives. Transformed cells were grown in 1 liter of Luria-Bertani medium, induced, harvested, and sonicated in buffer A (50 mM HEPES, pH 8.0, 5 mM $MgCl_2$, 0.1 mM EDTA, 10% sucrose) as described previously (5), except that the initial screenings were performed with 50-ml cultures. The purification was performed at 0 to 4°C. The crude extract was applied onto a 12-ml DEAE-Sepharose column (Pharmacia) equilibrated in buffer A and eluted with a linear NaCl gradient (10 column volumes, 0 to 0.5 M). The purest fractions were pooled, desalted, and concentrated. The enzymes were monitored by pyrophosphorolysis activity.

Iodine staining. The procedure for iodine staining (22) was modified as follows for cells growing in liquid media. Transformed *E. coli* BL21(DE3) cells with wild-type or mutated pETEC were inoculated onto 3 ml of Luria-Bertani medium and grown at 37°C until they reached an optical density at 600 nm of ~0.8. We added 1 mM isopropyl-β-D-thiogalactopyranoside and incubated the cells at room temperature for 30 min with shaking. We added glucose to a final concentration of 0.2% (wt/vol) and extended the incubation for 1 h. An aliquot of 0.1 ml was withdrawn and centrifuged in a 1.5-ml microcentrifuge tube at 14,000 rpm for 5 min. Supernatant was carefully aspirated to remove all liquid, leaving a compact pellet at the bottom of the tube. The microcentrifuge tube was turned upside down, and an iodine crystal was positioned in the cap of the tube (base), and the tube was closed. In 5 min, iodine vapor stained the cell pellet (top).

Enzyme assays. (i) Pyrophosphorolysis direction. The formation of [^{32}P]ATP from $^{32}PP_i$ and ADP-Glc was measured as described previously (43). The standard aqueous reaction mixture contained 50 mM HEPES buffer (pH 8.0), 7 mM

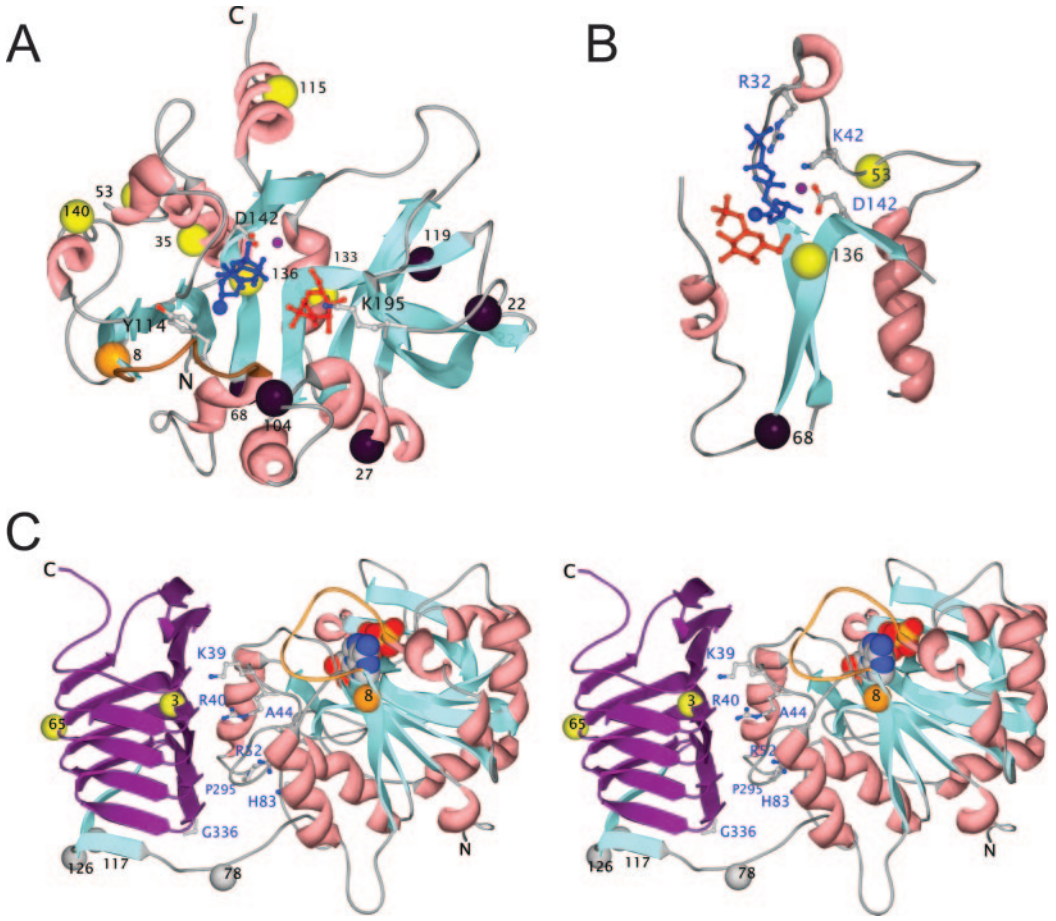

FIG. 1. Homology models of *E. coli* ADP-Glc PPase. Models were built as described in Materials and Methods. (A) The model was built on the known structure of dTDP-Glc PPase representing the N-terminal (catalytic) domain of the *E. coli* ADP-Glc PPase. Residues R32, K42, Y114, D142, and K195 are depicted as balls and sticks, and the protein structure is in a Richardson-style ribbon diagram. Yellow spheres represent pentapeptide insertions that disrupted the enzyme activity. Dark spheres are insertions that did not abolish the activity and stained with iodine. An orange sphere depicts an insertion that eliminated the activation by FBP. Modeled Glc1P is in red and deoxyribose triphosphate in blue. The oversized blue sphere in the deoxyribose triphosphate molecule represents where the adenine moiety would be covalently bound. The purple dot represents a modeled Mg^{2+}. (B) Selected elements of the structure in panel A are shown at a different angle. (C) Stereo diagram of the model with the N and C domains of the *E. coli* ADP-Glc PPase was based on the S subunit from the potato tuber enzyme. The protein structure is in a Richardson-style ribbon diagram, and the substrate ATP is in a space-filling representation. Yellow spheres represent insertions in the C domain that abolished the activity. White spheres are insertions that introduced stop codons. The purple structure is expressed as a separate polypeptide initiated in Met^{328} when a stop codon was introduced with insertion 117. The orange sphere represents insertion 8 that abolishes the effect of activator FBP. The orange loop is between residues Gln^{105} and Gly^{116}; the Gln^{105}-Gly^{116} sequence interacts with the adenine moiety of the ATP and is just after insertion 8. Side chains and C-α depicted are from residues that when subjected to mutagenesis altered the allosteric properties of either the enzyme from *E. coli* or *A. tumefaciens*.

$MgCl_2$, 1 mM $^{32}PP_i$ (300 to 1,500 cpm/nmol), 2 mM ADP-Glc, 10 mM NaF, and 0.2 mg/ml bovine serum albumin, plus enzyme in a total volume of 0.25 ml. Unless otherwise stated, the reaction mixture contained 1.5 mM FBP. After 10 min of incubation at 37°C, the reaction was terminated by the addition of 3 ml of cold 5% trichloroacetic acid. The [^{32}P]ATP formed was bound to activated carbon (15% Norite A in 100 mM PP_i). After washing the ATP-bound carbon with cold 5% trichloroacetic acid, [^{32}P]ATP was hydrolyzed by the addition of 1 N HCl and boiling for 10 min. The released radioactivity was measured in a scintillation counter.

(ii) Synthesis direction. The synthesis of ADP-[^{14}C]Glc from [^{14}C]Glc1P and ATP was measured by the method of Yep et al. (56). The standard aqueous reaction mixture contained 50 mM HEPES buffer (pH 8.0), 7 mM $MgCl_2$, 0.5 mM [^{14}C]Glc1P (800 to 1,000 cpm/nmol), 1.5 mM ATP, 1.5 U/ml inorganic pyrophosphatase, and 0.2 mg/ml bovine serum albumin, plus enzyme in a total volume of 0.2 ml. Unless otherwise stated, the reaction mixture contained 1.5 mM FBP. Reaction mixtures were incubated for 10 min at 37°C, and the reactions were terminated by heating in a boiling water bath for 1 min. The ADP-[^{14}C]Glc was then converted to [^{14}C]glycogen by the addition of glycogen synthase (from *E. coli*) and nonradioactive glycogen as a primer. Glycogen formed was precipitated and washed, and the radioactivity was measured in a scintillation counter.

(iii) Unit definition. In the above enzyme assays of pyrophosphorolysis direction and synthesis direction, one unit of enzyme activity is equal to 1 μmol of product, either [^{32}P]ATP or [^{14}C]ADP-Glc, formed per minute.

Calculation of kinetic constants. The kinetic data were plotted as initial velocity (v) versus effector concentration ([S]). A modified Hill equation (26), $v = V_{max}[S]^n/(S_{0.5}{}^n + [S]^n)$, where n is the Hill coefficient and the constant $S_{0.5}$ is the amount of substrate needed to obtain 50% of the maximum activity (V_{max}), was fit to the data to obtain the optimum parameters. Fitting was performed by the Levenberg-Marquardt nonlinear least-squares algorithm provided by the computer program Origin 5.0 (47). The activation curves were fitted with a similar modified Hill equation $v = v_0 + (V_{max} - v_0)[S]^n/(S_{0.5}{}^n + [S]^n)$. The parameter v_0 is the activity in the absence of activator, and $S_{0.5}$ was replaced by $A_{0.5}$, which is the amount of activator needed to obtain 50% of the maximal activation ($V_{max} - v_0$). The change in activation is the ratio V_{max}/v_0, the ratio between the activities in the presence and absence of saturated concentrations of

FBP. In all cases, the deviations by the Levenberg-Marquardt method were less than 15% (47).

RESULTS

Homology modeling. A homology model of the *E. coli* ADP-Glc PPase between residues 20 and 293 was obtained and correlated with the experimental structural information available. The dTDP-Glc PPase from *E. coli* was selected as a template because of the several lines of evidence that support the idea that NDP-sugar PPases share a common fold in their catalytic domain (3, 4, 16). The identity between the sequence of the *E. coli* ADP-Glc PPase and dTDP-Glc PPase is 23% (52/226 aligned residues). For that number of aligned residues (226 residues), 23% identity lays in the blurred limit of the "safe homology modeling zone" that practically guarantees that two sequences fold into the same structure (33). However, a very important factor in the template selection was that these two proteins share a very similar "environment" as defined previously (52). Template and query proteins catalyze the same chemical reaction, the pyrophosphorolysis of a nucleoside diphosphate sugar, using one identical substrate (Glc1P) and the other very similar (ATP and dTTP). In addition, fold recognition programs detected very significant hits with the dTDP-Glc PPases. The structure of the *E. coli* ADP-Glc PPase was detected to belong to the same superfamily of the NDP-sugar PPases by comparison to a library of hidden Markov models (20). This detection was very significant, with an E value of 5.2×10^{-61}. The GenTHREADER program also detected the dTDP-Glc PPases as the best candidate for homology modeling with an E value of 4×10^{-4}, which is highly significant and assures confidence.

The consistency of the model with biochemical data is crucial (52), and in this regard, the locations of important residues were in good agreement with the experimental information collected so far. For instance, residues Asp^{142} and Lys^{195}, which are the catalytic residue and Glc1P binding site (16, 27), overlap very well with the equivalent Asp^{111} and Lys^{163} from the template dTDP-Glc PPase. In the model, Tyr^{114} is located close to the ATP in the substrate site, which is in good agreement with previous chemical modification data (36, 37) (Fig. 1A). The 100% conserved residues in all sequenced bacterial enzymes having experimentally assayed catalytic activity are close to the substrate site (not shown). Therefore, the structure obtained was considered a good model of the catalytic domain organization and spatial arrangement of important residues. Since the model was based on dTDP-Glc PPase, which is not a regulated enzyme and is always present in an active conformation, the model most probably reflects the active form of the ADP-Glc PPase (Fig. 1B).

Recently, the crystal structure of one of the subunits of a plant ADP-Glc PPase, the tetrameric form (S_4) of the S (catalytic) subunit from potato tuber, was solved (30). This subunit has 32% identity with the *E. coli* enzyme, which implies that it could be a good template for modeling the relative positions of the N and C domains (Fig. 1C). However, the crystal structure was obtained in the presence of sulfate (30), an allosteric inhibitor of that enzyme, which made it unsuitable for modeling the active conformation of the *E. coli* enzyme. On the other hand, from this crystal structure it was shown that the S subunit from the potato tuber ADP-Glc PPase and dTDP-Glc PPase (accession numbers 1H5R and 1MC3, see Materials and Methods) share a common fold in their catalytic domains (4) despite binding different substrates. The latter confirms that the chosen templates with active conformations were appropriate for modeling the enzyme from *E. coli*.

Screening of pentapeptide-scanning mutants. To perform a structure-function relationship study of the *E. coli* ADP-Glc PPase, we investigated the effects of pentapeptide insertions at different positions in the enzyme and analyzed the results based on the homology model. All the mutated plasmids on the coding region were sequenced to find the exact locations of the 15-bp insertions (Fig. 2). Fourteen of the insertions encoded five amino acid residues extra in the polypeptide sequence. The other seven insertions (ins4, ins19, ins37, ins78, ins98, ins117, and ins126) created a stop codon that generated truncated versions of the enzyme (Fig. 2). In the first screening, cells of *E. coli* BL21(DE3) transformed with the mutated plasmids were grown in liquid media, spun down, and tested for their ability to synthesize glycogen (iodine staining) as described in Materials and Methods. Under the assayed conditions, only colonies with substantial ADP-Glc PPase activity synthesized enough glycogen to stain brown or black. The colonies that contained mutated enzymes with no detectable activity stained light yellow. A further test on crude extracts, performed in the pyrophosphorolysis direction, revealed that many of the insertions disrupted the ADP-Glc PPase activity. In addition, the activity assay in the absence of the activator FBP revealed that the Ins8 enzyme had defective allosteric properties and was insensitive to activation (Fig. 3 and 4).

Mutant Ins117 enzyme deserved comprehensive analysis, which has been published elsewhere (6). At first, it was thought to be a truncated ADP-Glc PPase, but further studies demonstrated that it produced a "nicked" version of the enzyme. Because of a Met-coding codon located closely downstream of the inserted stop codon, the C terminus was still coexpressed and formed a hetero-oligomeric active enzyme (6). The enzymes Ins53, Ins35, Ins140, Ins37, Ins136, Ins4, Ins19, Ins133, Ins98, and Ins115 did not stain with iodine, and they did not have significant activity in crude extracts over the background. Except for these inactive mutants, all enzymes were partially purified to analyze the apparent affinities for substrates and activator and obtain more accurate kinetic information.

Insertions that produced defective allosteric properties. Ins3 and Ins65 enzymes were not very active in crude extracts compared to the control (Fig. 3), whereas the cells carrying them failed to positively stain with iodine. After purification, these forms showed a decreased apparent affinity for FBP. In the pyrophosphorolysis direction, Ins3 and Ins65 enzymes displayed 26- and 37-fold-higher $A_{0.5}$s for FBP than that of the wild-type enzyme, respectively (Table 1).

The most dramatic effect of all the insertions was obtained with ins8. FBP increases the substrate apparent affinities in the wild type, but it had only very small effects on the $S_{0.5}$ values exhibited by the Ins8 enzyme for Glc1P, ATP, ADP-Glc, and PP_i (Table 2). The main difference between this and other mutants with defective regulatory properties was that the activity of Ins8 enzyme in the absence of activator was similar to that exhibited by the wild type under the same assay conditions. FBP had no detectable effect on the Ins8 enzyme when

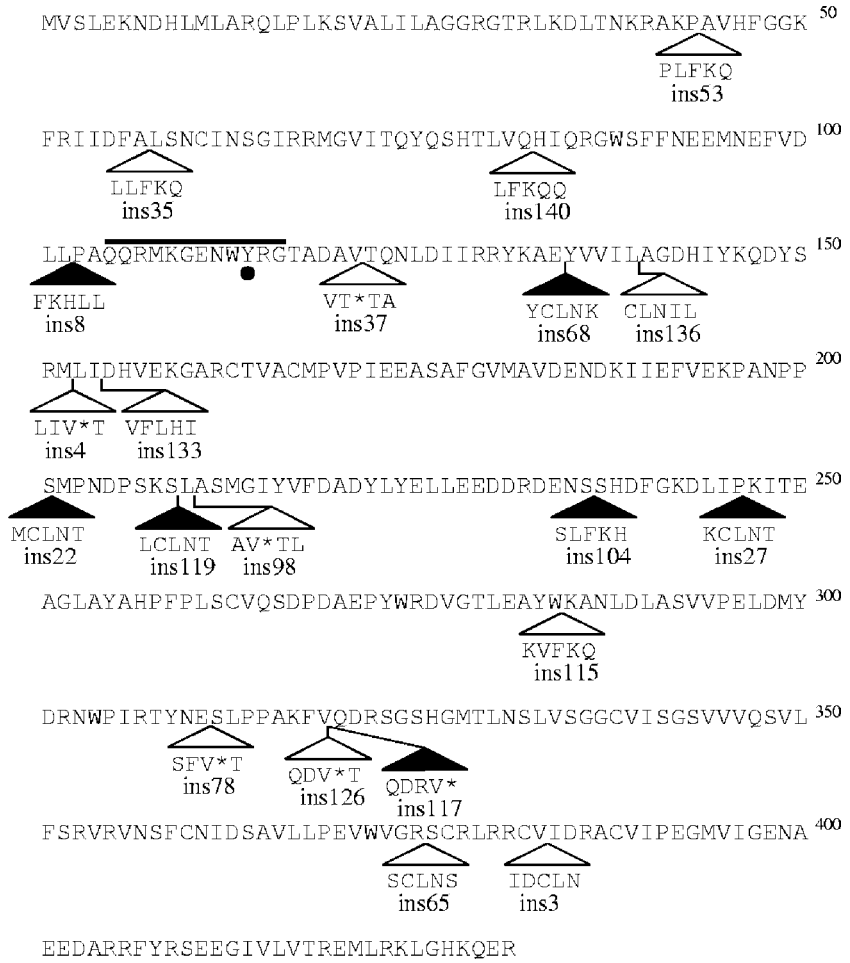

FIG. 2. Insertions in the *E. coli* ADP-Glc PPase gene. White triangles represent insertions that lead to transformed colonies that did not stain with iodine. Black triangles represent insertions in colonies that synthesized glycogen as detected by brown or black staining of the cells. The black line indicates a loop Gln^{105}-Gly^{116} that is predicted to interact with ATP. The black circle indicates Tyr^{114}, which was shown to be close to the ATP site. ins19 was not included in the figure, because it is equivalent to ins4; they had the same sequence.

assayed up to 10 mM (data not shown). Ins8 also had a low affinity for ATP, similar to what observed with the wild type assayed in the absence of FBP, but this may be an indirect effect from the lack of activation of the mutant. FBP increases the apparent affinity of the wild-type ADP-Glc PPase for ATP or ATP-Mg (Table 2 and Fig. 4), but Ins8 enzyme was completely insensitive to FBP, either to increase the catalytic rate or to increase the apparent affinity for ATP or ATP-Mg (Table 2 and Fig. 4). The lack of allosteric properties of the Ins8 enzyme was additionally supported by results obtained with respect to the inhibition exerted by AMP. It has been reported that ADP-Glc PPase from *E. coli* is inhibited by AMP, with studies showing interaction between the inhibitor and the activator FBP (18). For instance, 0.5 mM AMP inhibited the wild-type enzyme by about 30% or 90% when assayed in the ADP-Glc synthesis direction in the absence or in the presence of FBP (2.5 mM), respectively. The same concentration of AMP inhibited the Ins8 enzyme only about 20%, regardless of the presence of the allosteric activator, further indicating that the region surrounding Leu^{102} plays a critical role in the regulation of the enzyme.

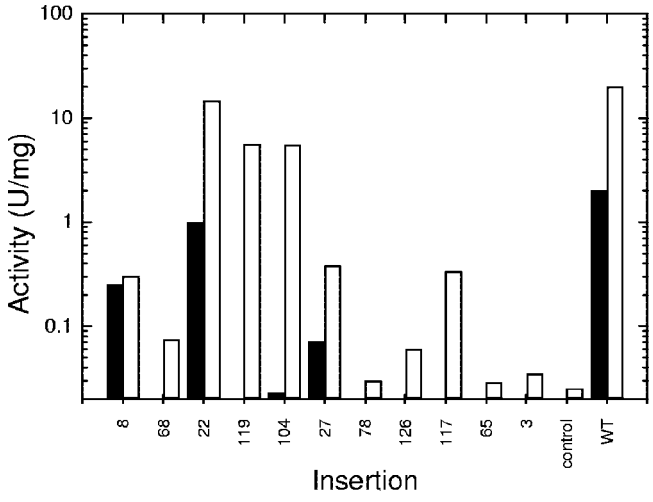

FIG. 3. Effect of FBP on the activity of different insertion mutants in crude extracts. Insertion mutants were expressed, and crude extracts were obtained as described in Materials and Methods. Aliquots were assayed in the pyrophosphorolysis direction as described in Materials and Methods in the presence of 1.5 mM FBP (white bars) or in the absence of activator (black bars). WT is the wild-type enzyme expressed with pETEC, and the control is pET24a without insert.

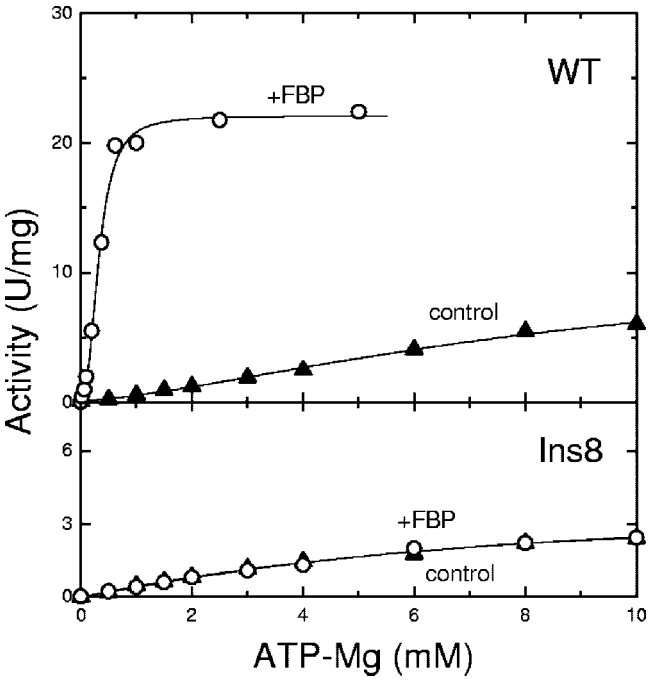

FIG. 4. Effect of FBP on the apparent affinity for ATP-Mg. Enzyme assays in the synthesis direction of the wild-type enzyme (WT) and Ins8 enzyme were performed as described in Materials and Methods. The concentration of $MgCl_2$ was 7 mM in the absence of ATP. Variations of ATP were accompanied by equimolar additions of $MgCl_2$ to ensure saturating concentration of free Mg^{2+} (7 mM). The concentration of FBP was 1.5 mM (white circles), whereas the control reaction mixtures (black triangles) did not contain FBP.

Insertions in the ATP subdomain. The N-terminal (catalytic) domain of the ADP-Glc PPase model has a central large open pocket that binds the nucleotide and sugar phosphate (Fig. 1A). The pocket can be divided into two sides or lobes as has been described for other pyrophosphorylases (8). The first lobe consists of residues 1 to 142 and encompasses residues interacting with the nucleotide (defined here as the ATP subdomain; Fig. 1A, left half). The second lobe contains residues 143 to 276 and encompasses residues interacting with the sugar moiety (Glc1P subdomain; Fig. 1A, right half). Analysis of the insertions was grouped according their locations in these two subdomains.

Ins68 and Ins136 enzymes had characteristics that were different from each other despite the close proximity of the insertions. Ins68 enzyme stained with iodine, whereas Ins136 enzyme had no detectable activity and did not stain. This agrees with the location of insertion 136 at position 140, only two residues apart from Asp^{142}, which has been previously described as having a critical role in catalysis (16). Even though insertion 68 was five residues upstream from insertion 136, it did not disrupt catalysis, and the apparent affinity for substrates was not seriously compromised. On the other hand, Ins68 enzyme was significantly more dependent on the activator FBP (Table 1). Insertion 68 may cause spatial arrangements which favor a more inhibited conformation of the enzyme because the apparent affinity for FBP decreased 5- and 10-fold in the synthesis and pyrophosphorolysis directions, respectively (Table 1). These results suggest a certain degree of tolerance to the structural modification of the insertion position and agree with the *E. coli* ADP-Glc PPase model. In the model, insertion 68 was away from the substrate site and at the N end of a β-sheet, whereas insertion 136 directly faced the substrate site at the C end of the same β-sheet near a catalytic residue and directly facing the substrate site (Fig. 1B).

Ins53 enzyme had negligible activity, in agreement with the fact that the insertion was in a loop in direct contact with the substrate site (Fig. 1B). In addition, insertion 53 fell two residues after Lys^{42}, which is equivalent to a residue (Lys^{43}) that is critical for activity in the S subunit of the potato tuber ADP-Glc PPase (2). Ins35, Ins140, and Ins115 enzymes, with no detectable activity, all had insertions located in α-helices (Fig. 1A). Moreover, insertion 140 was just before His^{83} (Fig. 1C), an important residue for the stability of the enzyme (28).

TABLE 1. Activation by FBP of the insertion mutants in the direction of ADP-Glc synthesis and pyrophosphorolysis

Enzyme[a]	FBP activation of insertion mutant in the direction of[b]:							
	ADP-Glc synthesis				Pyrophosphorolysis			
	$A_{0.5}$ (mM)	n	Activation (fold)	V_{max} (U/mg)	$A_{0.5}$ (mM)	n	Activation (fold)	V_{max} (U/mg)
Wild type	0.065	1.8	50	10.1	0.025	1.7	9.9	18.7
Ins3	0.95	1.5	>200[c]	0.11	0.650	1.9	>100[c]	0.10
Ins8	N/A[d]	N/A	N/A	0.43[e]	N/A	N/A	N/A	1.29[e]
Ins22	0.43	1.2	35	5.81	0.270	1.5	12	9.20
Ins27	0.25	1.8	60	6.44	0.060	1.8	15	6.03
Ins65	1.10	1.9	>200	0.20	0.930	1.7	>100	0.15
Ins68	0.31	2.3	>200	0.63	0.210	1.8	>100	0.30
Ins78	0.77	1.9	150	0.23	0.330	1.6	40	0.26
Ins104	0.30	1.4	45	4.32	0.081	1.9	18	7.45
Ins119	0.51	1.7	>200	4.10	0.250	2.1	25	10.80
Ins126	0.81	1.7	135	0.43	0.330	1.7	37	0.54

[a] Enzymes were partially purified and assayed as indicated in Materials and Methods.
[b] Deviations of the four parameters, $A_{0.5}$, n, activation (fold), and V_{max}, were lower than 15%. $A_{0.5}$ is the amount of activator needed to obtain 50% of the maximal activation. V_{max} is the maximum activity. The Hill coefficient is n. Activation (fold) is the ratio between the activities in the presence and absence of saturated concentrations of FBP as defined in Materials and Methods.
[c] These values (>200 and >100) indicate that the enzymes showed very low activity in the absence of FBP.
[d] N/A, not applicable (activation by FBP was negligible, and constants could not be determined).
[e] Activity in the presence of 2.5 mM FBP was not significantly different from activity in the absence of activator.

TABLE 2. Kinetic parameters of the insertion mutants in the presence and absence of FBP in the direction of ADP-Glc synthesis or pyrophosphorolysis

Enzyme[a]	FBP concn (mM)	Synthesis[b]:				Pyrophosphorolysis[b]:			
		Glc1P		ATP		ADP-Glc		PP_i	
		$S_{0.5}$ (mM)	n	$S_{0.5}$ (mM)	n	$S_{0.5}$ (mM)	n	$S_{0.5}$ (mM)	n
Wild type	0	0.19	0.8	2.20	1.5	0.36	1.8	0.75	1.4
	1.5	0.038	1.0	0.35	1.7	0.10	2.0	0.21	1.2
Ins3	0	N/A[c]	N/A	N/A	N/A	N/A	N/A	N/A	N/A
	1.5	0.090	1.2	0.45	1.9	0.18	1.6	0.35	1.3
Ins8	0	0.440	0.8	7.20	1.1	0.29	1.4	0.77	1.1
	1.5	0.220	1.4	7.10	1.1	0.38	1.3	0.48	1.2
Ins22	0	2.10	1.0	1.70	0.6	0.57	1.7	0.70	1.6
	1.5	0.060	1.3	0.93	1.6	0.35	1.8	0.23	1.8
Ins27	0	1.70	1.2	1.10	1.8	0.70	1.9	0.81	1.4
	1.5	0.069	1.5	1.00	2.3	0.39	1.7	0.18	1.5
Ins65	0	N/A	N/A	N/A	N/A	N/A	N/A	N/A	N/A
	1.5	0.15	1.3	0.55	2.0	0.17	1.3	0.15	1.4
Ins68	0	N/A	N/A	N/A	N/A	N/A	N/A	N/A	N/A
	1.5	0.12	1.1	0.84	3.5	0.17	2.1	0.11	0.8
Ins78	0	0.25	1.0	1.85	1.8	0.35	1.5	0.85	1.3
	1.5	0.050	1.3	0.44	1.5	0.12	1.5	0.24	1.1
Ins104	0	2.55	1.2	1.00	1.2	0.75	1.6	0.90	1.2
	1.5	0.069	1.4	1.35	3.6	0.53	1.7	0.22	1.4
Ins119	0	N/A	N/A	N/A	N/A	0.47	0.8	0.33	1.6
	1.5	0.15	1.4	1.49	2.2	0.19	1.4	0.32	1.3
Ins126	0	0.24	0.9	2.75	1.8	0.34	1.9	0.75	1.2
	1.5	0.030	1.2	0.27	2.0	0.15	1.6	0.27	1.1

[a] Enzymes were partially purified and assayed as indicated in Materials and Methods.
[b] Deviations of the two parameters ($S_{0.5}$ and n) were lower than 15%. $S_{0.5}$ is the amount of substrate needed to obtain 50% of the maximum activity (V_{max}). The Hill coefficient is n, as defined in Materials and Methods.
[c] N/A, not applicable (the activity of the enzyme was negligible in the absence of FBP).

Insertions in the Glc1P subdomain. Enzyme forms Ins27 and Ins104 had insertions at neighboring positions. Both mutants stained with iodine, and their kinetic properties were not very different from those of the wild-type enzyme. The apparent affinity for FBP decreased only two- to fivefold in both cases (Table 1). The apparent affinities for Glc1P in the absence of activator were lower for both Ins27 and Ins104 enzymes, but FBP corrected this problem (Table 2). The biggest difference was the apparent affinity for ADP-Glc in the presence of the activator, which was fourfold lower for Ins27 and fivefold lower for Ins104. This area seemed to be tolerant of insertions and not very critical for enzyme function. Insertions 22 and 119 are closer to the Glc1P subdomain but are in loops away from the substrate site (Fig. 1A). The main effect of these insertions was a decrease of less than 1 order of magnitude in the apparent affinity for FBP (Table 1). In the absence of activator, the apparent affinity for Glc1P was 10-fold lower for the Ins22 enzyme, with the other kinetic parameters not significantly different from those of the wild type (Table 2).

Analysis of inserted stop codons. Most insertions that created a stop codon (ins37, ins4, ins19, ins98, ins78, and ins126) generated enzymes that produced colonies that failed to stain with iodine. The exception was ins117, which generated a nicked enzyme rather than a truncated enzyme (6). A truncated enzyme at this point was inactive, but coexpression of a translated C terminus (Met^{328}-Arg^{431}; Fig. 1C) restored activity (6). Cells with Ins78 and Ins126 enzymes did not stain, but their extracts had very low but detectable activity (Fig. 3). A residual coexpression of the C terminus (Met^{328}-Arg^{431}) must be contributing to this detected activity because a plain truncation in this region renders an inactive enzyme (6). Proteins with ins78 and ins126 insertions were purified and characterized (Tables 1 and 2), revealing properties for both proteins that were similar to those reported for Ins117 enzyme (6). The main difference between the wild-type enzyme and both Ins78 and Ins126 enzymes was that the apparent affinity for FBP decreased 12- to 13-fold (Table 1). This agrees with the data previously reported for Ins117 enzyme. Truncated enzymes Ins37, Ins4, Ins19, and Ins98 were even shorter versions than the truncated inactive enzyme examined by Bejar et al. (6). They were also inactive, confirming that both the N domain (residues 1 to ~320) and C domain (residues ~328 to 431) are needed to produce an active enzyme.

DISCUSSION

Interaction between the C and N domains was postulated to be important for allosteric regulation of ADP-Glc PPase from *E. coli* (5, 6). Here, a homology model of the enzyme highlights an interface with important regulatory residues between those domains (Fig. 1C). It has been reported that mutation of these residues changes the allosteric properties of the *E. coli* enzyme. Lys^{39} binds to pyridoxal 5′-phosphate, an analog of FBP and an activator of the enzyme (45). Mutation of this residue decreases the apparent affinity for FBP (17). Replacement of Ala^{44} and His^{83} yields enzymes with lower affinities for the activator (28, 41). On the other hand, mutation of Gly^{336} and Pro^{295} generates mutants in a preactivated state with higher apparent affinities for FBP (40, 42). Arg^{40} and Arg^{52} are equivalent to two important residues for activation of the *Agrobacterium tumefaciens* enzyme by fructose 6-phosphate (19). The presence of all these residues between the N and C domains indicate that this interface plays a critical role in the interaction of the enzyme with the activator. Not only residues in the N-terminal domain play a role in the interaction with the activator, but residues in the C terminus must interact too. Construction of chimeric enzymes demonstrated that the C terminus determines the specificity for activation by FBP (5). Also, other studies have shown that changes in amino acids located in the C terminus of the plant enzyme produce a shift in the activator preference from 3-phosphoglycerate to FBP (50) and that a motif outside the pyrophosphorylase domain is involved in subunit interaction (10).

Insertion of five amino acids has been shown to be very useful in mapping important regions in several proteins and uncovering hidden structure-function relationships (1, 9, 15, 24, 44). In this work, regions of *E. coli* ADP-Glc PPase containing insertions can be classified based on their effects. Insertions that generated mutant enzymes that did not stain with iodine and exhibited impaired activity fell at regions with lower tolerance for structural modifications, like secondary structure elements or functionally important loops. In contrast, insertions that generated mutants staining with iodine and displaying significant activity were in regions with better tolerance for local structural alteration and away from the substrate site. Overall, these results agree with the predicted structural model and validate it. The most interesting insertions were those affecting the allosteric behavior of the enzyme. In agreement with the idea that the C terminus is important for regulation, Ins3 and Ins65 enzymes had significantly reduced affinity for FBP. These insertion mutants have low activity in crude extracts because of the very low expression level, as detected by immunoblotting (not shown).

The most interesting insertion mutant was the Ins8 enzyme, which exhibited no activation of the ADP-Glc PPase from *E. coli* (Fig. 4). In the models, this insertion is at the end of a β-sheet and just before a loop (Gln^{105}-Gly^{116}) that is proposed to interact with the substrate ATP (Fig. 1C) in the same way as observed in the crystal structure of the S subunit of the potato tuber ADP-Glc PPase (30). This loop contains Tyr^{114}, which reacts with a photoreactive 8-azido-adenosine derivative of ATP, indicating that this residue is very close to the adenosine binding site. In addition, mutation of Tyr^{114} decreases the apparent affinity for ATP (34).

One of the main roles of FBP on the *E. coli* ADP-Glc PPase is to increase the apparent affinity for ATP and Mg^{2+} (21). Insertion 8 completely disrupts this effect, indicating that the area surrounding Leu^{102} is critical for allosteric activation and strongly suggesting that the loop Gln^{105}-Gly^{116} is involved in the mechanism. This area is not in the interface between the N and C domains but is in a neighboring loop (Fig. 1C). The involvement of the loop Gln^{105}-Gly^{116} in both the interaction with ATP and the activation by FBP explains why mutations on Tyr^{114} also affected the apparent affinity for FBP (34). Insertion 8 may be blocking the binding of the activator or, most probably, interrupting the communication between the allosteric site (interface between N-C domains) and the substrate (ATP) site. This insertion brought the focus of attention to the region around Leu^{102} to find key residues that trigger the allosteric activation after binding of FBP. Alanine-scanning mutagenesis of this region combined with binding experiments could elucidate important details of the mechanism of regulation of ADP-Glc PPase. Those experiments are under way.

ACKNOWLEDGMENTS

This work was supported in part by Department of Energy research grant DE-FG02-93ER20121, Northern Regional USDA grant NC1-142, and research grant IS-3733-05R from BARD, the United States-Israel Binational Agricultural Research and Development Fund (J.P.); ANPCyT (PICT'03 1-14733; PICTO/UNL'03 1-13241; PAV 137), CONICET, and Fundación Antorchas (Argentina) (A.A.I.); and start-up funds from the College of Arts and Sciences of Loyola University, Chicago, IL (M.A.B.).

REFERENCES

1. **Anton, B. P., and E. A. Raleigh.** 2004. Transposon-mediated linker insertion scanning mutagenesis of the *Escherichia coli* McrA endonuclease. J. Bacteriol. **186:**5699–5707.
2. **Ballicora, M. A., J. R. Dubay, C. H. Devillers, and J. Preiss.** 2005. Resurrecting the ancestral enzymatic role of a modulatory subunit. J. Biol. Chem. **280:**10189–10195.
3. **Ballicora, M. A., A. A. Iglesias, and J. Preiss.** 2003. ADP-glucose pyrophosphorylase, a regulatory enzyme for bacterial glycogen synthesis. Microbiol. Mol. Biol. Rev. **67:**213–225.
4. **Ballicora, M. A., A. A. Iglesias, and J. Preiss.** 2004. ADP-glucose pyrophosphorylase: a regulatory enzyme for plant starch synthesis. Photosynth. Res. **79:**1–24.
5. **Ballicora, M. A., J. I. Sesma, A. A. Iglesias, and J. Preiss.** 2002. Characterization of chimeric ADPglucose pyrophosphorylases of *Escherichia coli* and *Agrobacterium tumefaciens*. Importance of the C-terminus on the selectivity for allosteric regulators. Biochemistry **41:**9431–9437.
6. **Bejar, C. M., M. A. Ballicora, D. F. Gómez-Casati, A. A. Iglesias, and J. Preiss.** 2004. The ADP-glucose pyrophosphorylase from *Escherichia coli* comprises two tightly bound distinct domains. FEBS Lett. **573:**99–104.
7. **Biery, M. C., M. Lopata, and N. L. Craig.** 2000. A minimal system for Tn7 transposition: the transposon-encoded proteins TnsA and TnsB can execute DNA breakage and joining reactions that generate circularized Tn7 species. J. Mol. Biol. **297:**25–37.
8. **Brown, K., F. Pompeo, S. Dixon, D. Mengin-Lecreulx, C. Cambillau, and Y. Bourne.** 1999. Crystal structure of the bifunctional N-acetylglucosamine 1-phosphate uridyltransferase from *Escherichia coli*: a paradigm for the related pyrophosphorylase superfamily. EMBO J. **18:**4096–4107.
9. **Cao, Y. H., B. Hallet, D. J. Sherratt, and F. Hayes.** 1997. Structure-function correlations in the XerD site-specific recombinase revealed by pentapeptide scanning mutagenesis. J. Mol. Biol. **274:**39–53.
10. **Cross, J. M., M. Clancy, J. R. Shaw, S. K. Boehlein, T. W. Greene, R. R. Schmidt, T. W. Okita, and L. C. Hannah.** 2005. A polymorphic motif in the small subunit of ADP-glucose pyrophosphorylase modulates interactions between the small and large subunits. Plant J. **41:**501–511.
11. **Cupp-Vickery, J. R., R. Y. Igarashi, and C. R. Meyer.** 2005. Preliminary crystallographic analysis of ADP-glucose pyrophosphorylase from *Agrobacterium tumefaciens*. Acta Crystallogr. Sect. F **61:**266–268.
12. **Eisenberg, D., R. Luthy, and J. U. Bowie.** 1997. VERIFY3D: assessment of protein models with three-dimensional profiles. Methods Enzymol. **277:**396–404.
13. **Fiser, A., R. K. G. Do, and A. Sali.** 2000. Modeling of loops in protein structures. Protein Sci. **9:**1753–1773.

14. **Fiser, A., and A. Sali.** 2003. ModLoop: automated modeling of loops in protein structures. Bioinformatics **19:**2500–2501.
15. **Fransen, M., I. Vastiau, C. Brees, V. Brys, G. P. Mannaerts, and P. P. Van Veldhoven.** 2005. Analysis of human Pex19p's domain structure by pentapeptide scanning mutagenesis. J. Mol. Biol. **346:**1275–1286.
16. **Frueauf, J. B., M. A. Ballicora, and J. Preiss.** 2001. Aspartate residue 142 is important for catalysis by ADP-glucose pyrophosphorylase from *Escherichia coli*. J. Biol. Chem. **276:**46319–46325.
17. **Gardiol, A., and J. Preiss.** 1990. *Escherichia coli* E-39 ADPglucose synthetase has different activation kinetics from the wild-type allosteric enzyme. Arch. Biochem. Biophys. **280:**175–180.
18. **Gentner, N., and J. Preiss.** 1967. Activator-inhibitor interactions in the adenosine diphosphate glucose pyrophosphorylase of *Escherichia coli* B. Biochem. Biophys. Res. Commun. **27:**417–423.
19. **Gómez-Casati, D. F., R. Y. Igarashi, C. N. Berger, M. E. Brandt, A. A. Iglesias, and C. R. Meyer.** 2001. Identification of functionally important amino-terminal arginines of *Agrobacterium tumefaciens* ADP-glucose pyrophosphorylase by alanine scanning mutagenesis. Biochemistry **40:**10169–10178.
20. **Gough, J., K. Karplus, R. Hughey, and C. Chothia.** 2001. Assignment of homology to genome sequences using a library of hidden Markov models that represent all proteins of known structure. J. Mol. Biol. **313:**903–919.
21. **Govons, S., N. Gentner, E. Greenberg, and J. Preiss.** 1973. Biosynthesis of bacterial glycogen. XI. Kinetic characterization of an altered adenosine diphosphate-glucose synthase from a "glycogen-excess" mutant of *Escherichia coli* B. J. Biol. Chem. **248:**1731–1740.
22. **Govons, S., R. Vinopal, J. Ingraham, and J. Preiss.** 1969. Isolation of mutants of *Escherichia coli* B altered in their ability to synthesize glycogen. J. Bacteriol. **97:**970–972.
23. **Guex, N., and M. C. Peitsch.** 1997. SWISS-MODEL and the Swiss-PdbViewer: an environment for comparative protein modeling. Electrophoresis **18:**2714–2723.
24. **Hallet, B., D. J. Sherratt, and F. Hayes.** 1997. Pentapeptide scanning mutagenesis: random insertion of a variable five amino acid cassette in a target protein. Nucleic Acids Res. **25:**1866–1867.
25. **Hayes, F., and B. Hallet.** 2000. Pentapeptide scanning mutagenesis: encouraging old proteins to execute unusual tricks. Trends Microbiol. **8:**571–577.
26. **Hill, A. V.** 1910. The possible effects of the aggregation of the molecules of haemoglobin on its dissociation curves. J. Physiol. (London) **40:**4–7.
27. **Hill, M. A., K. Kaufmann, J. Otero, and J. Preiss.** 1991. Biosynthesis of bacterial glycogen. Mutagenesis of a catalytic site residue of ADP-glucose pyrophosphorylase from *Escherichia coli*. J. Biol. Chem. **266:**12455–12460.
28. **Hill, M. A., and J. Preiss.** 1998. Functional analysis of conserved histidines in ADP-glucose pyrophosphorylase from *Escherichia coli*. Biochem. Biophys. Res. Commun. **244:**573–577.
29. **Iglesias, A. A., and J. Preiss.** 1992. Bacterial glycogen and plant starch biosynthesis. Biochem. Educ. **20:**196–203.
30. **Jin, X., M. A. Ballicora, J. Preiss, and J. H. Geiger.** 2005. Crystal structure of potato tuber ADP-glucose pyrophosphorylase. EMBO J. **24:**694–704.
31. **Jones, D. T.** 1999. GenTHREADER: an efficient and reliable protein fold recognition method for genomic sequences. J. Mol. Biol. **287:**797–815.
32. **Jones, D. T.** 1999. Protein secondary structure prediction based on position-specific scoring matrices. J. Mol. Biol. **292:**195–202.
33. **Krieger, E., S. B. Nabuurs, and G. Vriend.** 2003. Homology modeling, p. 509–523. *In* P. E. Bourne and H. Weissig (ed.), Structural bioinformatics. Wiley-Liss, Inc., Hoboken, NJ.
34. **Kumar, A., T. Tanaka, Y. M. Lee, and J. Preiss.** 1988. Biosynthesis of bacterial glycogen. Use of site-directed mutagenesis to probe the role of tyrosine 114 in the catalytic mechanism of ADP-glucose synthetase from *Escherichia coli*. J. Biol. Chem. **263:**14634–14639.
35. **Laskowski, R. A., M. W. MacArthur, D. S. Moss, and J. M. Thornton.** 1993. Procheck—a program to check the stereochemical quality of protein structures. J. Appl. Crystallogr. **26:**283–291.
36. **Lee, Y. M., S. Mukherjee, and J. Preiss.** 1986. Covalent modification of *Escherichia coli* ADPglucose synthetase with 8-azido substrate analogs. Arch. Biochem. Biophys. **244:**585–595.
37. **Lee, Y. M., and J. Preiss.** 1986. Covalent modification of substrate-binding sites of *Escherichia coli* ADP-glucose synthetase. Isolation and structural characterization of 8-azido-ADP-glucose-incorporated peptides. J. Biol. Chem. **261:**1058–1064.
38. **McGuffin, L. J., K. Bryson, and D. T. Jones.** 2000. The PSIPRED protein structure prediction server. Bioinformatics **16:**404–405.
39. **McGuffin, L. J., and D. T. Jones.** 2003. Improvement of the GenTHREADER method for genomic fold recognition. Bioinformatics **19:**874–881.
40. **Meyer, C. R., J. A. Bork, S. Nadler, J. Yirsa, and J. Preiss.** 1998. Site-directed mutagenesis of a regulatory site of *Escherichia coli* ADP-glucose pyrophosphorylase: the role of residue 336 in allosteric behavior. Arch. Biochem. Biophys. **353:**152–159.
41. **Meyer, C. R., P. Ghosh, S. Nadler, and J. Preiss.** 1993. Cloning, expression, and sequence of an allosteric mutant ADPglucose pyrophosphorylase from *Escherichia coli* B. Arch. Biochem. Biophys. **302:**64–71.
42. **Meyer, C. R., J. Yirsa, B. Gott, and J. Preiss.** 1998. A kinetic study of site-directed mutants of *Escherichia coli* ADP-glucose pyrophosphorylase: the role of residue 295 in allosteric regulation. Arch. Biochem. Biophys. **352:**247–254.
43. **Morell, M. K., M. Bloom, V. Knowles, and J. Preiss.** 1987. Subunit structure of spinach leaf ADPglucose pyrophosphorylase. Plant Physiol. **85:**182–187.
44. **Narberhaus, F., and S. Balsiger.** 2003. Structure-function studies of *Escherichia coli* RpoH (σ^{32}) by in vitro linker insertion mutagenesis. J. Bacteriol. **185:**2731–2738.
45. **Parsons, T. F., and J. Preiss.** 1978. Biosynthesis of bacterial glycogen. Isolation and characterization of the pyridoxal-P allosteric activator site and the ADP-glucose-protected pyridoxal-P binding site of *Escherichia coli* B ADP-glucose synthase. J. Biol. Chem. **253:**7638–7645.
46. **Preiss, J., S. G. Yung, and P. A. Baecker.** 1983. Regulation of bacterial glycogen synthesis. Mol. Cell. Biochem. **57:**61–80.
47. **Press, W. H., B. P. Flannery, S. A. Teukolsky, and W. T. Vetterling.** 1988. Numerical recipes in C: the art of scientific computing. Cambridge University Press, New York, NY.
48. **Ramachandran, G. N., C. Ramakrishnan, and V. Sasisekharan.** 1963. Stereochemistry of polypeptide chain configurations. J. Mol. Biol. **7:**95–99.
49. **Rost, B.** 1996. PHD: predicting one-dimensional protein structure by profile-based neural networks. Methods Enzymol. **266:**525–539.
50. **Salamone, P. R., I. H. Kavakli, C. J. Slattery, and T. W. Okita.** 2002. Directed molecular evolution of ADP-glucose pyrophosphorylase. Proc. Natl. Acad. Sci. USA **99:**1070–1075.
51. **Sali, A., and T. L. Blundell.** 1993. Comparative protein modeling by satisfaction of spatial restraints. J. Mol. Biol. **234:**779–815.
52. **Sánchez, R., and A. Sali.** 2000. Comparative protein structure modeling. Methods Mol. Biol. **143:**97–129.
53. **Schwede, T., J. Kopp, N. Guex, and M. C. Peitsch.** 2003. SWISS-MODEL: an automated protein homology-modeling server. Nucleic Acids Res. **31:**3381–3385.
54. **Smith, P. K., R. I. Krohn, G. T. Hermanson, A. K. Mallia, F. H. Gartner, M. D. Provenzano, E. K. Fujimoto, N. M. Goeke, B. J. Olson, and D. C. Klenk.** 1985. Measurement of protein using bicinchoninic acid. Anal. Biochem. **150:**76–85.
55. **Strange, R. E.** 1968. Bacterial "glycogen" and survival. Nature **220:**606–6077.
56. **Yep, A., C. M. Bejar, M. A. Ballicora, J. R. Dubay, A. A. Iglesias, and J. Preiss.** 2004. An assay for adenosine 5′-diphosphate (ADP)-glucose pyrophosphorylase that measures the synthesis of radioactive ADP-glucose with glycogen synthase. Anal. Biochem. **324:**52–59.